# OPTIMAL PARAMETERS FOR FINITE DIFFERENCE MODELING OF 2D SEISMIC WAVE EQUATION

**B. Galuzzi[1], E. Stucchi[1], E. Zampieri[2]**
[1] *Dipartimento di Scienze della Terra "A. Desio", Università degli Studi di Milano, Italy*
[2] *Dipartimento di Matematica "F. Enriques", Università degli Studi di Milano, Italy*

**Introduction.** Full waveform inversion is a classical contest of data inversion in which the numerical solution of the wave equation is compared with one or more seismograms to obtain information on the Earth's subsurface (Tarantola, 1986), (Virieux and Operto, 2009). Consequently, accurate and efficient numerical implementation of the wave equation is still an active research field and involves sampling quantities such as time, space and physical properties of the subsurface, along with choosing an appropriate numerical method of resolution and writing an efficient resolution code. Approximation error and execution time determine the effectiveness of the implementation. An effective code exhibits the right balance between these two factors because the use of high-resolution parameters to decrease the approximation error causes a large execution time, which, for seismic inversion applications, should remain in the order of a few seconds or lower. For example it may be necessary to use about ten thousand or one hundred thousand synthetic seismograms to resolve a problem of seismic inversion by global optimization algorithms (Sajeva *et al*., 2014).

In this work we study the relationship between these two factors in the contest of the numerical solution of the 2D acoustic wave equation. The numerical solution is obtained from finite difference software, written at the University of Milan, in which the implementation parameters can be set in order to get an efficient solution. At the beginning we derive the 2D acoustic seismic wave equation and explain the numerical implementation and the parameters of modeling used. Then, we analyze which parameters cause the highest approximation error and find that they are the space step size and the order of approximation of space derivatives. We study their behavior in a simple constant-velocity model as a function of the maximum frequency of the source signal and we analyze the relation with the execution time. Finally, we apply these considerations on a complex-velocity model and find the right parameters of modeling to get the optimum trade-off between the approximation error and the execution time.

**The 2D acoustic seismic equation.** The seismic wave propagation in a geological medium is often modeled by the acoustic 3D equation (Fichner, 2010)

$$\frac{\partial^2 p(x,y,z,t)}{\partial t^2} = c(x,y,z)^2 \left( \frac{\partial^2 p(x,y,z,t)}{\partial x^2} + \frac{\partial^2 p(x,y,z,t)}{\partial y^2} + \frac{\partial^2 p(x,y,z,t)}{\partial z^2} \right) + f(x,y,z,t),$$

with $p$ acoustic pressure of the wave, f seismic source and c acoustic wave speed. A realistic range for wave speed can be between 1500 m/s (water) and 7000 m/s (granite). Since the seismic source has a space dimension much smaller than the geological medium, it can be approximated by a point source in space

$$f(x,y,z) = \delta(x-x_0)\delta(y-y_0)\delta(z-z_0)s(t),$$

where $s(t)$ is the seismic wavelet, describing the variation of seismic source in time. One important aspect of the modeling is the maximum frequency $f_{max}$ of the wavelet. Since many source-receiver geometries are often confined to a plane (for example $y$=0), it is possible to use the acoustic 2.5-D equation (Bleinstein, 1986)

$$\frac{\partial^2 p(x,y,z,t)}{\partial t^2} = c(x,z)^2 \left( \frac{\partial^2 p(x,y,z,t)}{\partial x^2} + \frac{\partial^2 p(x,y,z,t)}{\partial y^2} + \frac{\partial^2 p(x,y,z,t)}{\partial z^2} \right) + f(x,y,z,t),$$

which differs from the 3D equation only for the fact that $c$ varies only as a function of the depth $z$ and the length $x$. Finally, because of the large computational cost of 3D modeling, we consider the 2D acoustic wave equation

$$\frac{\partial^2 p(x,z,t)}{\partial t^2} = c(x,z)^2 \left( \frac{\partial^2 p(x,z,t)}{\partial x^2} + \frac{\partial^2 p(x,z,t)}{\partial z^2} \right) + \delta(x - x_0)\delta(z - z_0)s(t).$$

In general a 2D modeling of wave propagation cannot be used in general to make a direct quantitative comparison, including amplitude information, with seismic data acquired along a line and assumed to be 2.5-D, but there are many strategies that make the passage from 2D to 2.5-D possible (Liner, 1991; Williamson and Pratt, 1995; Song and Williamson, 1995).

**Modeling of the acoustic seismic equation.** In our numerical implementation of the acoustic wave equation we use an explicit finite difference method (Cohen, 2002), with uniform time step and uniform space step (with the same step for depth and length). In order to approximate the time and space derivatives we use different finite difference operators.

We implement a second order operator to approximate the time-derivative

$$\frac{\partial^2 p(x,z,t)}{\partial t^2} = \frac{p(x,z,t+dt) - 2p(x,z,t) + p(x,z,t-dt)}{dt^2} + O(dt^2),$$

and implement a 2n-order space operator to approximate the space derivatives

$$\frac{\partial^2 p(x,z,t)}{\partial x^2} = \frac{\sum_{i=1}^{n} c_i \left( p(x+idx,z,t) + p(x-idx,z,t) \right)}{dx^2} - 2\frac{(\sum_{i=1}^{n} c_i) p(x,z,t)}{dx^2} + O(dx^{2n}),$$

$$\frac{\partial^2 p(x,z,t)}{\partial z^2} = \frac{\sum_{i=1}^{n} c_i \left( p(x,z+idz,t) + p(x,z-idz,t) \right)}{dz^2} - 2\frac{(\sum_{i=1}^{n} c_i) p(x,z,t)}{dz^2} + O(dz^{2n}),$$

where the $c_i$ are the coefficients for the 2n-order of approximation of derivatives (Cohen, 2002). Tab. 1 lists the values of $c_i$, obtained as a function of the order of approximation $ord_s=2n$, for some values of $n$.

Tab. 1 - Values of the coefficients for different order of approximation of spatial derivative.

| ords | c1 | c2 | c3 | c4 | c5 | c6 |
|---|---|---|---|---|---|---|
| 2 | 1 | 0 | 0 | 0 | 0 | 0 |
| 4 | 4/3 | -1/12 | 0 | 0 | 0 | 0 |
| 6 | 3/2 | -3/20 | 1/60 | 0 | 0 | 0 |
| 8 | 8/5 | -1/5 | 8/135 | -1/560 | 0 | 0 |
| 10 | 5/3 | -5/21 | 5/126 | -5/1008 | 1/3150 | 0 |
| 12 | 12/7 | -15/56 | 10/189 | -1/112 | 2/1925 | -1/16632 |

In the interest of computational efficiency, the limitation of the computational domain to only a part of the true physical domain introduces reflecting boundaries that do not exist. We use the Gaussian taper method (Cerjan *et al.*, 1985) to suppress the undesired reflections, in which we introduced a thin absorbing region along the artificial boundary where the wave field is attenuated.

**Approximation error of the implementation.** There are four main parameters that influence the approximation error of the implementation: the time step *dt*, the space step *dx*, the order of approximation of the space operator $ord_s=2n$ and the size of the absorbing region, expressed as the number of grid nodes. To focus the attention only on the first three parameters, we can choose an absorbing region so large as to make irrelevant the error introduced by the boundaries of the model. There are two main relations between these three parameters. The first is numerical stability (Courant *et al.*, 1967)

$$dt < \frac{dx}{c_{max}} \lambda,$$

with $\lambda=\lambda(ord_s)\in[0.5,1]$, that is the Courant number. This relation limits the maximum possible

Tab. 2 - Values of $n$ as a function of ords, to obtain an error below 1%.

| $ord_s$ | 2 | 4 | 6 | 8 | 10 | 12 | 14 | 16 | 18 | 20 | 22 | 24 |
|---|---|---|---|---|---|---|---|---|---|---|---|---|
| $n$ | 18 | 6.3 | 4.5 | 3.75 | 3.5 | 3.25 | 3 | 2.9 | 2.8 | 2.7 | 2.6 | 2.5 |

time step as a function of the space step size $dx$ and the maximum velocity $c_{max}$. The second is the numerical dispersion (Alford *et al.*, 1974)

$$dx < \frac{c_{min}}{f_{max} n},$$

where $n=n(ord_s)$ is the number of points per wavelength. Grid dispersion limits the maximum possible space step by the minimum velocity cmin and the maximum frequency $f_{max}$ of the source signal $s(t)$. We consider the function $\cos\left(\frac{2\pi x}{l}\right)$, where $l$ denotes the wavelength, to estimate the values of n. If we calculate the second derivative of this function analytically at $x=0$, and we set $l=1$, we obtain $-4\pi^2$. The numerical solution can be obtained by sampling the function with different sampling intervals $dx=l/n$, where $n$ is the number of points per wavelength and by using different 2n-order operators. Tab. 2 lists the values of $n$, as a function of the order of approximation $ord_s$, to obtain an error below 1%.

Numerical stability is a necessary condition to implement any explicit finite difference method. Because of the order of magnitude of the wave speed in rocks, the stability condition implies that the maximum possible time step must be approximately three order of magnitude at least lower than the minimum possible space step size $dt_{max} \approx 10^{-3} dx_{min}$; if this condition is met, the error of approximation is more sensitive to spatial parameters ($dx$,$ord_s$). For this reason, we study the error of approximation and execution time as a function of $dx$ and $ord_s$.

**A constant-velocity test.** To simulate a simple seismic acquisition, we consider a rectangular region with dimensions X=3240 m and Z=1620 m, with a constant velocity of $c=1500$ m/s (water velocity). We choose a seismic source located in $(x_0, z_0)=(27\text{ m}, 27\text{ m})$, characterized by a Ricker wavelet

$$s(t) = (1 - 2a(t - t_0)^2)e^{-a(t-t_0)^2},$$

with $a=\pi^2 f_0^2$ and $t_0=0.2$ *s*. The choice of this wavelet is so because it is simple to control its maximum frequency, that is $f_{max} \approx 3 f_0$. The recording spread is composed of 119 receivers, equally spaced by 27 m, with a depth of 27 m and also an offset of 27 m to the first receiver. In the case of constant velocity model without boundary, the solution of the equation is (Aki and Richards, 2002)

$$p(x,z,t) = \frac{1}{2\pi c^2} \int_0^{t^s} \frac{s\left(t - \frac{\sqrt{(x-x_0)^2 + (z-z_0)^2 + s^2}}{c}\right)}{\sqrt{(x-x_0)^2 + (z-z_0)^2 + s^2}} ds,$$

with $t_s$ that depends on the duration of the wavelet, usually much smaller than the duration of registration $T$. If we use a quadrature formula to approximate the integral, we have a solution of the problem whose accuracy is independent of distance and time, but depends only on the accuracy of the quadrature formula. This procedure allows building an "exact" solution that can be compared with our numerical solutions (we can consider our model as unbounded using a large absorbing boundary condition). A numerical implementation of this problem was made with a fixed time step of $dt=0.0005$ s and a recording length of $T=2s$. To study the behavior of the approximation error and execution time, we consider two different grid cell size $dx$=[27 m, 9 m], twelve different space orders of approximation $ord_s$=[2,4…24] and three different wavelets with $f_s$=[5 Hz, 10 Hz, 15 Hz] (which correspond to $f_{max}$=[15 Hz, 30 Hz, 45 Hz]). To compare the numerical solution with the "exact" solution, we use the following measure of

numerical error:

$$err = \frac{1}{temp * nric} \sum_{i=1}^{temp} \sum_{j=1}^{nric} |real_{i,j} - sint_{i,j}|,$$

where *temp*=4000 is the number of time samples, *nric*=119 is the number of receivers, $real_{i,j}$ is the "exact" seismogram and $sint_{i,j}$ is the numerical one. Both seismograms are normalized to their maximum value.

Fig. 1a shows the six curves (two for each frequency $f_s$) of the approximation error as a function of $ord_s$. It is possible to see that the error increases with *dx* and $f_{max}$, according to the relation of grid dispersion. We note also that the curves of approximation decrease, in general with $ord_s$, but this behavior depends also on *dx* and $f_{max}$. In particular, for frequency $f_{max}$=45 Hz (the green curves), we note that the curve with *dx*=27 m slowly decreases as a function of $ord_s$, while the one with *dx*=9 m decreases fast until $ord_s \approx 8$. Then we notice that the error remains stable around $5*10^{-5}$. Similarly, for frequency $f_{max}$=30 Hz (the blue curves), the curve with *dx*=27 m slowly decreases as a function of $ord_s$, while the one with *dx*=9 m decreases fast until $ord_s$=6. Here the error remains stable around $2.5*10^{-5}$. Finally, for frequency $f_{max}$=15 Hz (the red curves), the curve with *dx*=27 m decreases fast as a function of $ord_s$ until $ord_s$=8 and then remains stable around an error of $2*10^{-4}$, while the curve with *dx*=9 m, decreases fast until $ord_s$=6, it remains nearly constant until $ord_s$=12 and finally increases slowly. Overall it remains stable around an error of $1*10^{-5}$. Therefore the whole behavior of the curves does not appear to be simple. However, for high frequencies, the better way to reduce the error is to decrease *dx* and slightly increase $ord_s$. Increasing only the order of approximation $ord_s$ seems to bring only minor improvements. Instead, for low frequencies, there is no need to use short step sizes: *dx*=27 m with $ord_s \approx 8$ gives a sufficiently low approximation error, without the necessity to further increase $ord_s$. For middle frequencies, the error appears to be more complex. However, using a short *dx* with a low $ord_s$ is a good compromise, while an equally valid solution is to use a high order of approximation $ord_s$ with higher space step sizes *dx*.

The behavior of modeling as a function of *dx*, $ord_s$ and $f_{max}$ can be explained by the grid dispersion relation. If we place $c_{min}$=1500 m/s and $f_{max}$=45 Hz, (green curves in Fig. 1a) we obtain

$$n < \frac{33.3}{dx}.$$

Therefore, if we want to use a space step size with *dx*=9 m (the dashed green curve in Fig. 1a) it is sufficient to have $n \approx 3.7$, which corresponds from Tab. 2 to an $ord_s \approx 8$; greater order of approximation will not produce significant improvements, because the curve remains almost

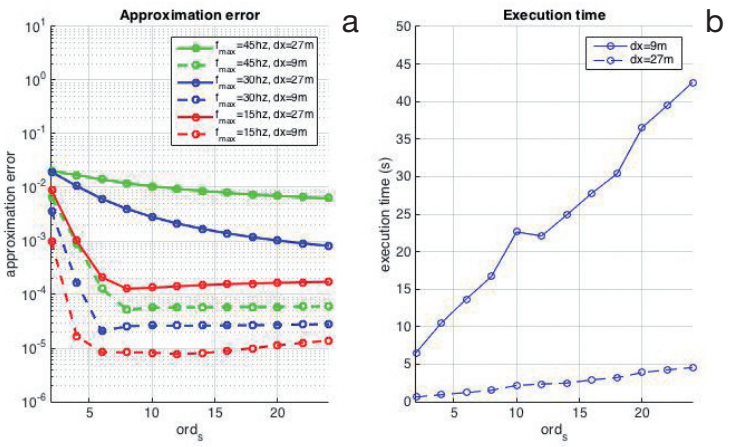


Fig. 1 – Approximation error (left) and execution time (right) for different modeling parameters.

constant. On the contrary, if we want a space step size of $dx$=27 m (the continuous green curve), it would be necessary that $n\approx1.2$. However, this is not possible because of the Nyquist theorem and consequently the solution will have a great numerical dispersion. If we place $c_{min}$=1500 m/s and $f_{max}$=15 Hz, (red curves in Fig. 1a) we obtain

$$n < \frac{100}{dx}.$$

Therefore, if we want to use a space step size of $dx$=9 m, (the dashed red curve) it is sufficient to have $n\approx11.1$, which corresponds from Tab. 2 to $ord_s\approx4$; a greater order of approximation will not produce significant improvements because the error remains almost constant hereafter. On the contrary, if we need to use a space step of size $dx$=27 m, we must set $n\approx3.7$, so it will be necessary a higher order $ord_s$.

As a final consideration the error, especially for low $dx$, seems to converge to a low constant value different from zero for each maximum frequency. This is due to the fact that the error related to time discretization takes over when the error related to space discretization decreases. This error is low for low maximum frequency $f_{max}$, and increases with $f_{max}$.

In addition to this consideration about approximation error, it is important to evaluate the execution time. In Fig. 1b we represent the two execution time curves, in function of $ord_s$, related to $dx$=[27 m, 9 m] with $f_{max}$=15 Hz (for different maximum frequency the execution time did not change). We can note that execution time increases in function of $dx$ and $ord_s$. In particular the curve with $dx$=27 m is always below that with $dx$=9 m. This is due to the numerical method implemented, since we have

$$T \propto nx * nz * ord_s$$

where $T$ is the execution time and $nx$*$nz$ is the number of grid nodes.

Then, the execution time increases quadratically as a function of $dx$ and only linearly with $ord_s$. Therefore it can be more convenient to increase $ord_s$ rather than decreasing $dx$, to obtain comparable error but with a lower execution time. As an example, the modeling with $dx$=9 m and $ord_s$=4 has an error comparable with the modeling with $dx$=27 m and $ord_s$=24. Moreover the first has an execution time of 11 s, while the second of only 5 s.

**A complex-velocity test.** We simulated another seismic acquisition with the same parameters of acquisition as the previous one: one point source, the same numbers of receivers, a registration time of $T$=2 s and a time step $dt$=0.0005 s. We now assumed that the velocity varies as a function of the depth and length $c$=$c$ ($x$, $z$) (Fig. 2a), with a range between 1500 m/s and about 4500 m/s. This velocity model is a readjustment of a portion of the Marmousi model

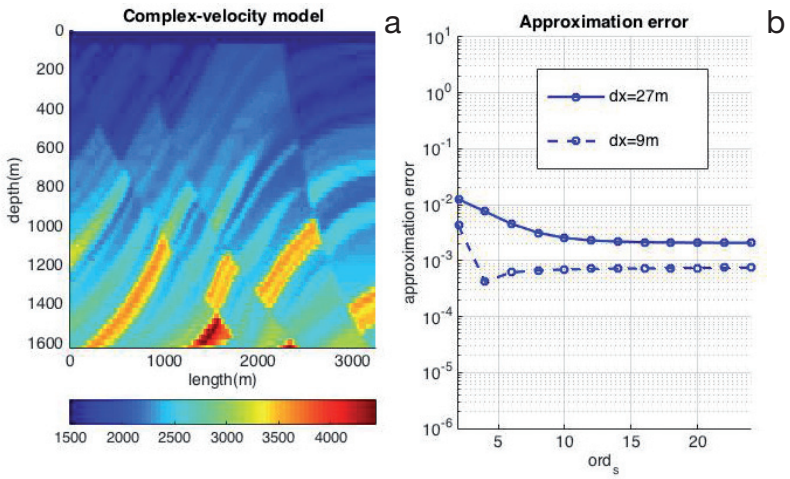


Fig. 2 – Complex-velocity model (left) and its approximation error (right).

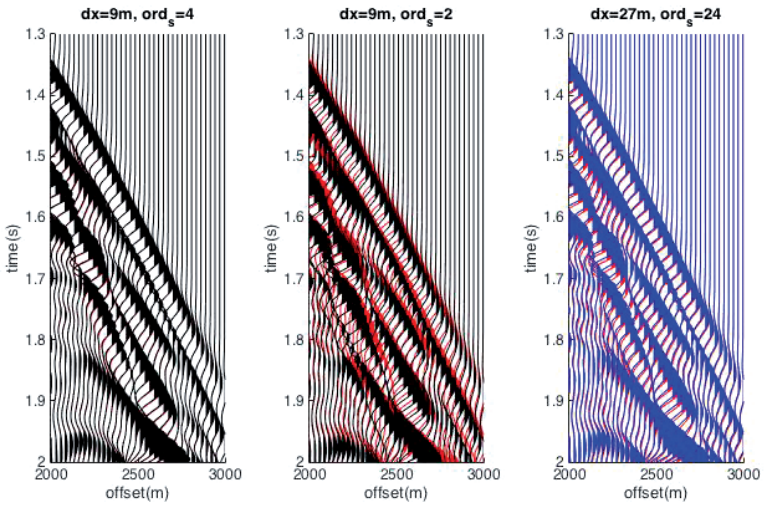


Fig. 3 – Three portions of three different seismograms for different modelling parameters. On the left $dx$=9 m, $ord_s$=4. In the center $dx$=9 m, $ord_s$=2. On the right $dx$=27 m, $ord_s$=24. All of them are confronted with the exact seismograms, in red.

(Bourgeois *et al.*, 1991). We considered absorbing boundary conditions for lateral and bottom sides. On the contrary, for the topside we considered a reflective boundary condition (expressed by $p(x, 0,t)=0, \ \forall\ x, t$) to simulate the high contrast of velocity and density between air and water. For this modeling there is not an exact solution to be compared with the numerical ones. So as "exact" solution we use a numerical one with $dx$=1 m, $dt$=0.000125 s and $ord_s$=4. To study the behavior of error and execution time, we consider again two different grid cell size $dx$=[27 m, 9 m], twelve different space orders of approximation $ord_s$=2,4…24 and a wavelet Ricker with $f_s$=10 Hz ($f_{max}$=30 Hz). The two execution time curves as a function of $ord_s$ are the same of Fig. 1b (execution time is not influenced by the velocity $c$), while the two curves of error are represented in Fig. 2b.

The behavior of these curves is similar to that of the previous test, but the error is higher. Indeed there are more seismic events in the seismogram for this test (reflected and refracted arrivals) than in the previous one. The curve of $dx$=27 m decreases slowly as a function of $ord_s$, while the one of $dx$=9 m decreases fast until $ord_s$=4, with the error remaining stable. We can note that, also in this case, it can be more convenient to use a space step of $dx$=27 m with high order $ord_s$, rather then a space step of $dx$=9 m and low $ord_s$. The errors we obtained in fact are comparable, but the execution time of the first case is lower (Fig. 1b).

In Fig. 3 we reported a portion of three numerical seismograms we obtained. The first, on the left, is the seismogram obtained with $dx$=9 m and $ord_s$=4, that corresponds to the better solution obtained with $dx$=9 m. The second, in the center, is the seismogram obtained with $dx$=9 and $ord_s$=2. The third, on the right, is the seismogram with $dx$=27 and $ord_s$=24, that corresponds to the best solution obtained with $dx$=27. All of them are confronted with the "exact solution" (the red seismograms on the graphics). We note that the third seismogram is better than the second one and, from Fig. 1b, it also has a lower execution time. On the other hand the first seismogram is better than the third one, even if the differences are not so pronounced, but it has a higher execution time. Therefore it can be more convenient to choose the modeling parameters used to compute the third seismogram instead of using the modeling parameters of the first one, especially if a huge number of forward modeling is required.

**Conclusions.** Using a constant velocity model and a portion of the Marmousi model, we studied the 2D acoustic seismic wave equation and the parameters of modelling necessary to implement an efficient numerical solution as a function of approximation error and execution time. The approximation error depends on the stability condition and the grid dispersion relation. We found that under the stability condition, the approximation error is above all influenced by the space step size $dx$ and the order $ord_s$ of the finite difference approximation of spatial

derivatives. Therefore an optimal trade-off between these two parameters is required in order to reduce the approximation error.

This approximation error can also be analysed in terms of the grid dispersion relation and therefore in terms of the ratio between the minimum velocity cmin in the model and the maximum frequency $f_{max}$ of the wavelet. If the ratio is low, it is necessary to use a low spatial step size and a medium order of spatial derivative approximation (for instance: $dx$=9 m and $ord_s$=6,8). If the ratio is high, it is possible to use a greater spatial step size, but with a higher order of spatial approximation (for instance: $dx$=27 m and $ord_s$=22,24). As a final consideration, if there are combinations of these two parameters that cause comparable errors, it is convenient to use the one with the greater space step size to reduce the execution time, especially in application such as the Full Waveform Inversion where a large number of forward modelling may be needed.

## References


Williamson, P. R., & Pratt, R. G. (1995). A critical review of acustic wave modeling procedures in 2.5D dimensions. *Geophysics , 60*, 591-595.

Virieux, J., & Operto, S. (2009). An overview of full waveform inversion in exploration geophysics. *Geophysics* , 127-152.

Aki, K., & Richards, P. G. (2002). *Quantitative Seismology* (2nd ed.). University Science Books.

Alford, R. M., Kelly, K. R., & Boore, D. M. (1974). Accuracy of finite difference modeling of the acoustic wave equation. *Geophysics , 39* (6), 834-842.

Bleinstein, N. (1986). Two-and-One-Half Dimensional in-Plane Wave Propagation. *Geophysical Prospecting , 34*, 686-703.

Bourgeois, A., Bourget, M., Lailly, P., Ricarte, P., & Versteeg, R. (1991). Marmousi, model and data. *European Association of Exploration Geophysicists*.

Cerjan, A., Kosloff, D., Kosloff, R., & Reshef, M. (1985). A non reflecting boundary condition for discrete acoustic and elastic wave equations. *Geophysics , 50*, 705-708.

Courant, R., Friedrichs, K., & Lewy, H. (1967, March). On the partial difference equations of mathematical physics. *IBM Journal* , 215-234.

Cohen, G. (2002). *Higher-order Numerical Methods for Transient Wave Equations*. Berlin: Springer-Verlag.

Fichner, A. (2010). *Full Seismic Waveform Modelling and Inversion*. Berlin: Springer-Verlag.

Liner, C. L. (1991). Theory of a 2.5-D acoustic wave equation for constant density media. *Geophysics , 56* (12), 2114-2117.

Sajeva, A., Aleardi, M., Galuzzi, B. G., Mazzotti, A., & Stucchi, E. M. (2014). Comparison of stochastic optimization methods on analytic objective function and on 1D elastic fwi. *European Association of Geoscientis and Engineers Conference and Exhibition*, (pp. 1893-1903). Amsterdam.

Song, Z., & Williamson, P. R. (1995). Frequency-domain acoustic wave modelling and inversion of crosshole data; Part 1, 2.5-D modelling method. *Geophysics , 60* (3), 784-795.

Tarantola, A. (1986). A strategy for nonlinear elastic inversion of seismic reflection data. *Geophysics , 51*, 1893-1903.